Development of an Innovative Protection System against Explosions for Concrete Structures

David Monteiro Nabais

Extended Abstract

Supervisor
Professor Doutor Eduardo Nuno Brito Santos Júlio
Major de Engenharia Gabriel de Jesus Gomes

October 2016

1. Introduction

Terrorism is a constant and eminent concern for any country. The damages that its manifestations provoke, by using explosives, have a catastrophic magnitude, affecting international instability and spreading chaos and panic among the populations. In a very significant form, an explosion affects all the elements around it, becoming lethal several times.

Therefore, the protection of infrastructures with higher explosion risk, becomes a priority. This master dissertation aims to develop an explosion protection system for concrete structures, following the research line of the inquiry design Security and Integrity of Strategical Infrastructures face a Accidental or Provoked Explosions (SI4E).

The study conducted was based on a reinforced concrete (RC) slab/element. Different concrete layers were used to strengthen the latter, using Ultra-High Performance Fiber Reinforced Concrete (UHPFRC), Light Weight Aggregate Concrete (LWAC) and Rubberized Concrete (RuC). In the experimental part, four RC slabs/walls, with 2.00 m of width and a height of 2.60 m where tested. The reference slab had a total thickness of 0.12 m, whereas for the remainders this parameter varied between 0.14 and 0.21 m.

2. 'Explosion' action

An explosion can be defined as a "transformation realised over a short period of time, in which a high quantity of gases and energy is released, usually as heat" (cit. Gomes, 2013). According to UFC 3-340-02 (2014), the explosions in the condensed phase can be categorized in two main groups: confined and unconfined explosions. These, in turn, can be subdivided based on the location of explosion charge and on confining degree.

Depending on the relative position of the explosion in relation to the target-structure, the unconfined explosions can be divided in to: (1) free-air burst, (2) air burst, (3) ground burst, (4) fully vented, (5) partially confined and (6) fully confined. In Figure 1, a scheme with blast loading categories is presented.

In this master thesis, only free-air burst are analysed in more detail, because they are the type of explosion observed in the study case. In this study, the blast wave propagates from the centre, reaching the structure without suffering any type of amplification due to reflections.

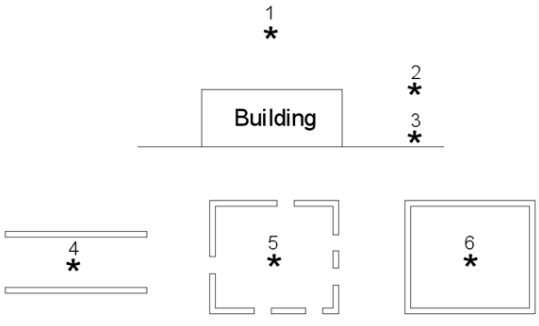

Figure 1 - Blast loading categories, adapted from UFC 3-340-02(2014)

2.1 Blast phenomena description

2.1.1 Scaling Method

The use of scalar quantities allows to study, to analyse and to analytical compare the results of blast waves, from different explosive mass and distances (Mlakar and Barker, 2010). Therefore, in order

to characterize the blast waves from a certain explosion and, consequently, the realized energy, it is common to scale the wave blasts' parameters by the root cubic of the explosive quantity, defined by Hopkinson-Cranz, according to equation (2.1):

$$Z = \frac{R}{\sqrt[3]{W}} \tag{2.1}$$

where *Z* is the scaled distance, *R* is the distance to the centre of explosion (in meters) and *W* is the mass of explosive charge (in kg).

2.1.2 TNT equivalency

Though the use of the scaling method allows the comparison of all the different parameters of wave blasts from different explosions, it is based on the explosion's energy and the reference explosive's mass, which, in this case, is Trinitrotoluene (TNT). Since not all the explosives release the same amount of energy per mass unit, it is common to characterize the explosion by its TNT equivalency, so it is possible to compare explosions caused by different types of explosives. This method is based on the calculation of a TNT charge, capable of producing the same explosion energy, wave blast and impulse as the explosive being studied (Mlakar and Barker, 2010).

The TNT equivalency, according to the heat of detonation of the various materials, can be represented by the equation (2.2) (UFC 3-340-02, 2014):

$$W_E = \frac{H_{EXP}^d}{H_{TNT}^d} * W_{Exp} \tag{2.2}$$

where:

W_E - effective charge weight;

W_{EXP} - weight of the explosive in question;

H_{Exp}^d - heat of detonation of explosive in question;

H_{TNT}^d – heat of detonation of TNT.

2.1.3 Blast wave

In order to describe the behaviour of a blast wave, it is necessary to define, at least, three parameters. The first one corresponds to the intensity of the initial impact, which is defined by the peak overpressure (P_{so}). The second parameter corresponds to the duration of the positive phase (t_0). The last one is the specific impulse due to positive and negative phases (Kinney and Graham, 1985).

After a detonation, a wave blast is formed and it propagates radially through the atmosphere. The arrival time of a wave blast at a certain point is measured from the centre of the explosion, and it is defined by t_a. At this instant, the pressure abruptly rises to a value named peak overpressure (P_{so}), after which a decay back to the ambient pressure (P_a) occurs in an infinitesimal period of time t_0. After the positive phase of a wave blast, a negative one occurs, with a duration of t_o^-, usually much longer than t_0, characterized by a negative pressure (lower to the ambient pressure), with a maximum value of P_{so}^- (UFC 3-340-02, 2014). Usually, unconfined explosions do not take into account the negative phase, since its intensity is much lower than the positive's intensity in absolute value. Furthermore, it has a reverse effect to the one that is generated by the blast in positive the phase, being conservative to not taking into account this effect to quantify the explosions' action in buildings (Remennikov, 2007). In Figure 2, an illustration of the described phenomena are presented.

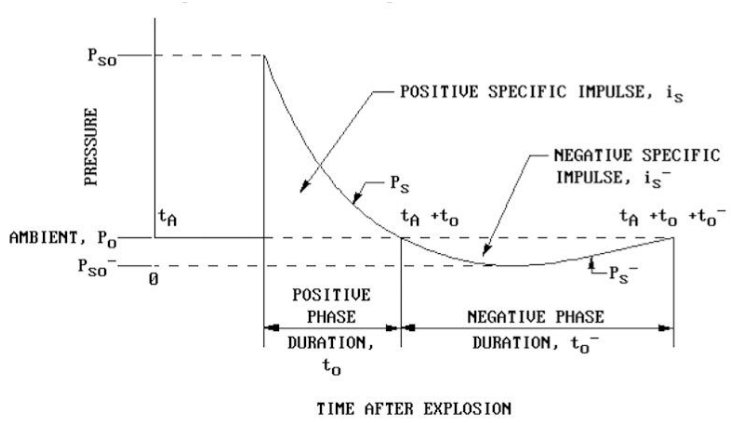

Figure 2 - Graphic Pressure-Time, adapted from UFC 3-340-02 (2014)

The peak overpressure (P_{so}) can be calculated according to equation (2.3), which is proposed by Kinney and Graham (1985).

$$P_{so} = \frac{808 \cdot \left[1 + \left(\frac{Z}{4,5}\right)^2\right] \cdot P_a}{\sqrt{1 + \left(\frac{Z}{0,048}\right)^2} \cdot \sqrt{1 + \left(\frac{Z}{0,32}\right)^2} \cdot \sqrt{1 + \left(\frac{Z}{1,35}\right)^2}} \text{ [MPa]} \tag{2.3}$$

The Department of Defence USA has established an empirical relation to estimate the peak overpressure, which is available within the interval 39,670 m/kg$^{1/3}$ (100 ft/lb$^{1/3}$) > Z > 0,0524 m/kg$^{1/3}$ (0,132 ft/lb$^{1/3}$) (UFC 3-340-02, 2014). In Figure 3, a comparison between the obtained results from different authors is presented.

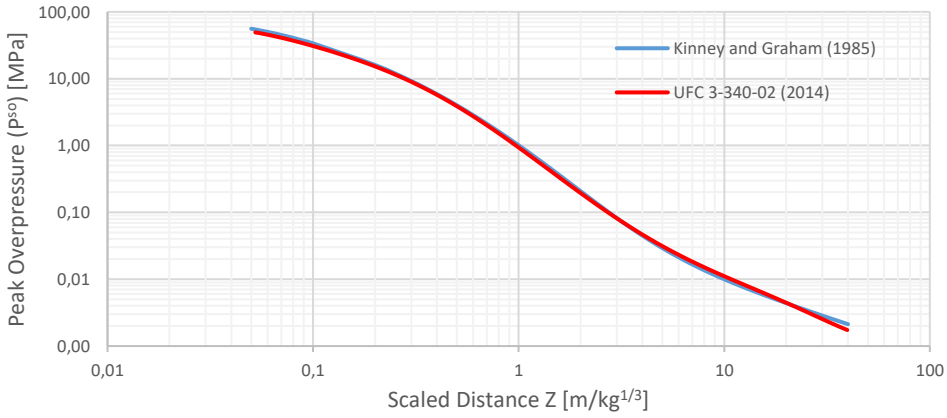

Figure 3 - Peak overpressure (P_{so})

The specific impulse is important data for the characterization of the explosion causing several damages. This parameter takes into account the peak overpressure and the positive phase's duration, and it can be obtained by the area below or above the curve of Figure 2, to the specific positive (i_s^+) or negative impulse (i_s^-), respectively (Kinney and Graham, 1985). Kinney and Graham (1985) have proposed an empirical equation to calculate the specific positive impulse:

$$i_s^+ = \frac{0,0067 \cdot \sqrt{1 + \left(\frac{Z}{0,23}\right)^4}}{Z^2 \cdot \sqrt[3]{1 + \left(\frac{Z}{1,55}\right)^3}} \text{ [MPa} \cdot \text{ms]} \tag{2.4}$$

Similarly to the peak overpressure, the UFC 3-340-302 (2014) has also established an empirical relation of the specific positive impulse to the scaled distance. In Figure 4, the results obtained by these two authors are presented. As can be observed, the results are quite similar.

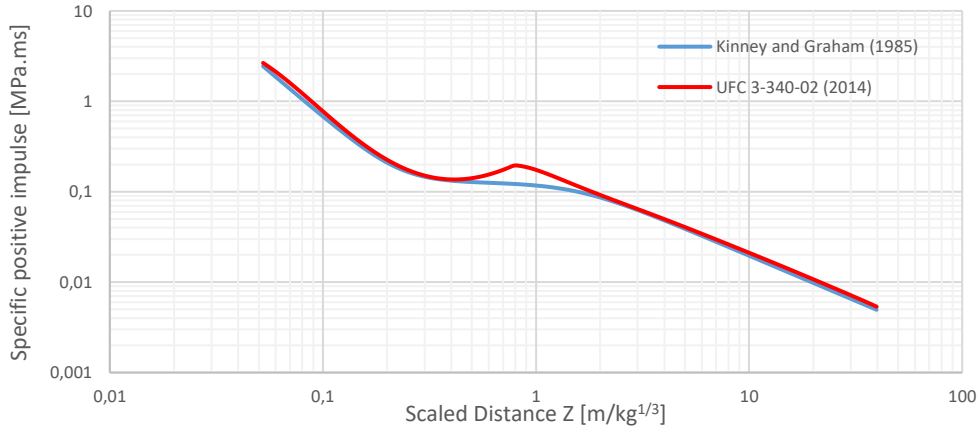

Figure 4 - Specific positive impulse (i_s^+)

2.1.4 Reflection

The interaction between the blast wave and the surface of a structure can be quite complex, because it depends on the way that the blast wave reaches that surface and on its geometry.

The normal reflection occurs when a shock wave strikes perpendicularly to a surface. After the wave reaches the surface, it is reflected in an opposite way, creating overpressure, until the value of peak reflected overpressure (P_r) is reached. In Figure 5, a reflected overpressure over the incident pressure can be observed. It should be noticed that the duration of positive and negative phases do not vary.

$$P_r = 2 \cdot P_{so} \cdot \left(\frac{7 \cdot P_a + 4 \cdot P_{so}}{7 \cdot P_a + P_{so}} \right) \text{ [MPa]} \tag{2.5}$$

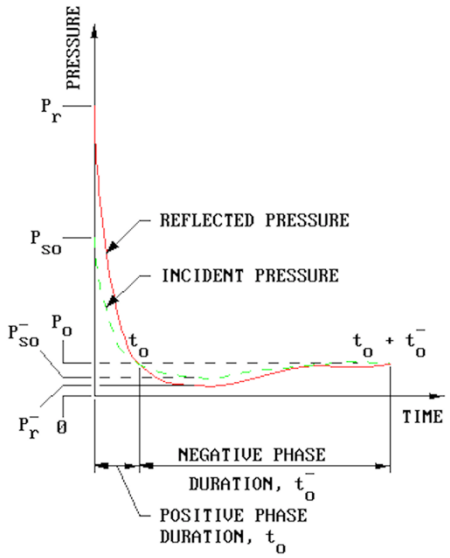

Figure 5 - Graphic of Pressure-Time to a free-air burst, adapted from UFC 3-340-02 (2014)

2.2 Dynamic analysis method

The analysis of the response of a structure to the actions of an explosion must be done taking into account a dynamic analysis of the process, since it is an effect with a brief duration (around milliseconds) when compared to the response time of a structure.

The simplest model used to make a design of a structure to explosive loads is the single degree of freedom (SDOF). To transform a real system into a SDOF, it is necessary to affect the load, the mass and the resistance of the structural element with the transformation factors, K_L, K_M e K_R. In order to simplify the calculation, it is common to use a transformation factor for the loading and mass, K_{LM}.

Besides these transformation factors, the materials' properties also have to be modified, since the materials do not have the same behaviour when submitted to dynamic loads or to static or quasi-static actions. The dynamic increase factors (DIFs) are those defined by the ratio between the dynamical properties of the material and its static properties, and they depend on the type of material, as well as on the type of the behaviour analysed (bending, diagonal tension, direct shear, etc.) (UFC 3-340-02, 2014). In Table 1, a few examples of DIFs can be observed.

Table 1 - Dynamic increase factors to reinforced concrete (adapted from UFC 3-340-02, 2014)

Type of stress	*Steel*	*Concrete*
Bending	*1.17*	*1.19*
Diagonal tension	*1.00*	*1.00*
Direct shear	*1.10*	*1.10*
Compression	*1.10*	*1.12*

Along with DIFs applied to the materials' properties, it is necessary to take into account the steel capacity to reach large deformations, keeping the same level of tension. Thus, UFC 3-340-02 (2014) has proposed the use of a strength increase factor (SIF) to the steel, equal to 1.10.

By applying the energetic methods, it is possible to estimate the deforming capacity of a structure due to the absorption of kinetics energy from a dynamic load. Equalizing the work induced by an external force (T_e) to the interior work (T_i) produced from the element's deformation, it is possible to approximately analyse the resulting deformation.

According to UFC 3-340-02 (2014), the external work can be calculated using the equation (2.6):

$$\mathrm{T_e} = \frac{\mathrm{i_r^2}}{2 \cdot \mathrm{m}} \tag{2.6}$$

Assuming that the structure behaves in an elastic-plastic regime, the relation between load and displacement can be represented by Figure 6, where y_e and y_m represent the elastic and plastic deformation, respectively.

The internal work (T_i) can be estimated taking into account the area below the resistance function, which results in equation (2.7):

$$\mathrm{T_i} = \frac{\mathrm{p_u} \cdot \mathrm{y_e}}{2} + \mathrm{p_u} \cdot (\mathrm{y_m} - \mathrm{y_e}) = \mathrm{p_u} \cdot \left(\mathrm{y_m} - \frac{1}{2}\mathrm{y_e}\right) \tag{2.7}$$

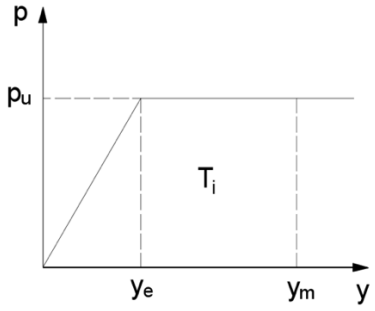

Figure 6 - Relation between load-displacement to an elastic-plastic regime

Balancing the external and the internal work, it is possible to obtain the equation (2.8), which is the most used equation to calculate the impulsive response of a system:

$$T_e = T_i \rightarrow \frac{i_r^2}{2 \cdot m} = p_u \cdot \left(y_m - \frac{1}{2} y_e\right) \tag{2.8}$$

In the calculation of stiffness of a structure, when submitted to an impulsive action, the moment of inertia considered in the calculation takes into account the cracking of the section. According to a UFC 3-340-02 (2014), the moment of inertia can be estimated using the equation (2.9):

$$I = \frac{I_g + I_c}{2} \tag{2.9}$$

where I_g *and* I_c are the moment of inertia of the gross concrete cross section and the moment of inertia of cracked concrete cross section, respectively. These values, to slabs, can be estimated by the equations (2.10) and (2.11):

$$I_g = \frac{h^3}{12} \tag{2.10}$$

$$I_c = F \cdot d^3 \tag{2.11}$$

where h is the thickness of gross concrete cross section, *d* is the distance from extreme compression fiber to centroid of tension reinforcement, and *F* is the coefficient of geometrical percentage of reinforcement taking into account the homogenization coefficient of the section.

The ultimate moment capacity of the section to an impulsive loading can be estimated by the equation (2.12) (Lúcio and Ramos, 2015):

$$M_{r,din} = \rho \cdot f_{y,din} \cdot d^2 \cdot \left(1 - \frac{\rho \cdot f_{y,din}}{2 \cdot f_{c,din}}\right) \tag{2.12}$$

where:

d - distance from extreme compression fiber to centroid of tension reinforcement;

ρ - geometric percentage of reinforcement;

$f_{y,din}$ - dynamic design stress for reinforcement;

$f_{c,din}$ - dynamic ultimate compressive strength of concrete.

3. Concrete

To reinforce the slabs used in the present study case, three different types of concrete were used. The layer closest to the slab, and corresponding to the first layer of reinforcement, was the ultra-high performance fibber reinforced concrete (UHPFRC), in order to create a more resistant layer and to minimize the damages inflicted on the structure. This type of concrete has certain mechanical properties, as compressive and diagonal tension, much higher than a plain concrete and, due to its dense matrix and reduced porosity, also has higher durability (Eide and Hisdal, 2012; Ayub *et al*., 2014).

In the middle layer, light weight aggregate concrete (LWAC) was used, which is a lighter and more porous material (Chen and Liu, 2008; Costa, 2012), in order to absorb part of the energy from the blast wave. The last layer was rubberized concrete (RuC), which directly receives the wave blast, so that these aggregates could dissipate part of the energy from the blast wave. However, since the aim of these layers is to dissipate energy, it is interesting to use a type of concrete with a high percentage of these aggregates (Valadares and Brito, 2010; Duarte *et al*. 2016). Another important factor is the

durability of this material, since it is the most exposed layer. The increase of the rubber percentage also affects this concrete's durability, as it becomes more permeable, allowing aggressive agents to be embedded in the concrete's matrix (Ganjian *et al.,* 2009; Gupta *et al.*, 2016).

Therefore, a protective layer with different materials was achieved, in which each material has a different function, but the same aim: to protect the structure against explosions.

4. Preparation of Tests

The test scheme used in this study is based on the work developed by Gonçalves (2015), in which the slab is placed on a two pinned support, in order to simulate a structure pinned support, with a hanging load above the centre of the slab, as represented in Figure 7. In this study, 20 cartridges of 230 g of military explosive PE4A were used, which make a total of 4.60 kg, with the following dimensions: 0.20 m x 0.15 m x 0.12 m.

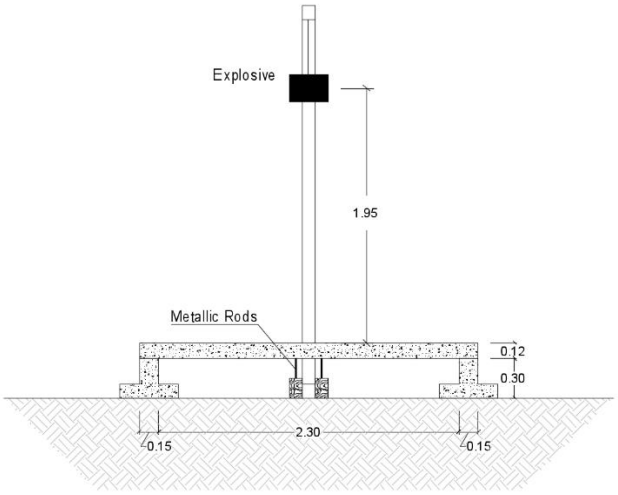

Figure 7 - Test scheme

In this study, four slabs with 2.00 m of width and 2.60m of length were tested; they were produced with concrete C25/30, inferior reinforcement of A500NR with $\emptyset 6$ // $0{,}125\ m$ and a 2.50 cm covering. The reference slab is 0.12 m thick; the first reinforced slab has a reinforced UHPFRC layer of 0.02 m, adding up to a total thickness of 0.14 m. The second reinforced slab, besides the 0.02 m of UHPFRC, has a layer of 0.04m of LWAC, thus with a total thickness of 0.18 m. Finally, the third reinforced slab, besides all the described layers, has a superficial layer of 0.03 m of RuC, having a total thickness of 0.21 m. The obtained results by a analytical analysis are presented in Table 2.

Table 2 - Obtained results by a analytical analysis

	M_r $[kNm/m]$	p_u $[kN/m^2]$	I $[m^4/m]$	K_e $[kN/m^2/m]$	y_e $[mm]$	y_m $[mm]$	$Test\ mesures$ $[mm]$
Reference Slab	*13.67*	*18.22*	*76.1x10^{-6}*	*5031*	*3.6*	*66.8*	*67.5*
UHPFRC Slab	*17.18*	*22.90*	*121x10^{-6}*	*8299*	*2.8*	*43.6*	*51.3*
UHPFRC + LWAC Slab	*17.18*	*22.90*	*258x10^{-6}*	*13998*	*1.6*	*37.4*	*42.6*
UHPFRC + LWAC + RuC Slab	*17.18*	*22.90*	*410x10^{-6}*	*20079*	*1.1*	*33.7*	*42.0*

5. Analysis and discussion of the results

By observing Table 2, it is possible to understand that the reinforcement layers have obtained maximum displacement lower than the ones of the reference slab and that, as the layers were added, the registered values have decreased. The observed damages on the reference slab were the most severe. However, with the addition of reinforcing layers, these damages have decreased and in the case of the two last reinforced slabs, the reinforcing layers were partially destroyed. Therefore, it is possible to conclude that these layers have absorbed part of the wave blast energy. The obtained results by a analytical analysis are closer to the registered values, with an error lower than 20%. In spite of this value being high, it is an approximated method, with the representation of a structure equivalent to a single degree of freedom. Thus the obtained error is acceptable. In the case of the two last reinforced slabs, the LWAC and RuC layers were made with the aim of dissipating energy. Thus distance *d* is only considered until the UHPFRC layer, therefore making the resistant capacities of these three reinforced slabs to be unchanged.

One way to understand the contribution of each reinforcement layer, besides the comparison with the reference slabs' results, is to compare them with one slab, with the same thickness of each reinforced slabs, composed just with C25/30 concrete. Figure 8, presents a graphic with the measured results and the analytical analysis of the four tested slabs and of slabs with the same thickness composed only with C25/30 concrete.

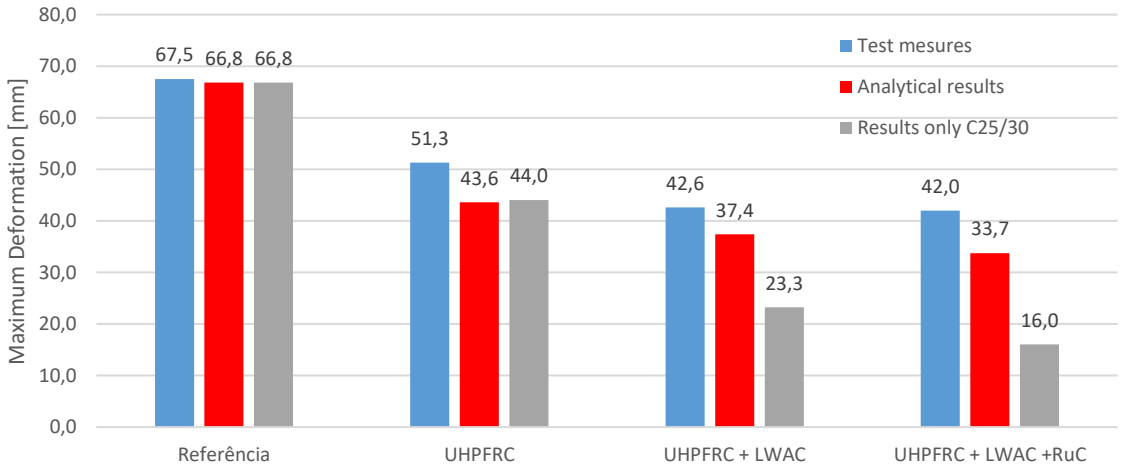

Figure 8 - Comparison between measures, analytical results and analytical results just with C25/30

The analytical analysis of the reinforced slab with UHPFRC has a better performance that the same thickness of slab composed only of C25/30 concrete. However, this improvement is not significant, because it is a less than 1 mm displacement. Concerning the reinforced LWAC and RuC slabs, there is significant improvement in the maximum displacement. The analytical analysis of the slab composed with only C25/30 concrete suggests an improvement of displacement, by 14.1 mm and 17.7 mm, respectively, to the second and third reinforced slabs.

This fact supports the assumption of the using of the LWAC and RuC layers to dissipate energy. Through energetic balance, the external work (T_e) produced by an explosion has to be balanced by the internal work (T_i) regenerated by that structure. As the energy dissipated by a concrete layer increases,

the generated T_i rises and, consequently, the registered displacements increase. On the other hand, when the blast wave's reflection on the element augments, the transmitted energy decreases and, therefore, displacement will be reduced. The external work is directly connected to the density of the target-structure. Thus, as density increases, hardness of the element also increases and displacement will be smaller, which corresponds to a bigger reflection of the blast wave.

6. Conclusions

An explosion is a complex phenomenon, with an extremely short duration in time (milliseconds), making its analysis a true challenge. The exponential decay of the incident pressure in time and distance is one of the most important subjects to understand the behaviour of this action, making possible to conclude that the most efficient protection system of concrete structures from explosions corresponds to ensuring that they are at a proper security distance from a possible explosion.

The used reinforcement layers enhance the slabs' performance to explosions. The maximum displacements registered, as well as the observed damages, have decreased with the increment of reinforcement layers. However, this decrease was not linear and a analytical analysis comparison to a slab, with the same thickness of each reinforced slab, composed with C25/30 concrete, has revealed that its behaviour was not the expected one. The maximum displacement of the reinforced slabs with LWAC and RuC, during the tests, were higher than the obtained displacement by the analytical analysis of the slabs (with the same thickness) composed only by C25/30 concrete. These results confirm that the use of these layers is adequate to dissipating energy, since through energetic balance, when the dissipated energy by a single layer of concrete increases, the T_i generated on the structure rises and, consequently, displacements of that element will be higher.

Considering the analytical analysis and the energetic balance, the LWAC and RuC layers will be an interesting choice to protect structures against confined explosions. By dissipating energy, the shock wave reflection decreases, leading to a lower amplification of its effects.

References

Ayub, T.; Shafiq, N.; Nuruddin, M. F. (2014), "*Mechanical Properties of High-Performance Concrete Reinforced with Basalt Fibers*", Procedia Engineering, V. 77, pp 131-139.

Chen, B.; Liu, J. (2008), "*Experimental application of mineral admixtures in lightweight concrete with high strength and workability*"; Construction and Building Materials, V. 22, No. 4, pp. 655-659.

Costa, H. S. S. (2012), "*Structural Lightweight Aggregate Concrete. Precast and Structural Reinforcement Applications"* (in Portuguese), Doctoral Dissertation in Civil Engineering, Faculty of Sciences and Technology, Coimbra University.

Duarte, A. P. C.; Silva, B. A.; Silvestre, N.; Brito, J.; Júlio, E.; Castro, J. M. (2016), "*Tests and Design of Short Steel Tubes Filled With Rubberised Concrete*", Engineering Structures, V. 112, pp. 274-286.

Eide, M. B.; Hisdal, J. M. (2012), "*Ultra High Performance Fibber Reinforced Concrete (UHPFRC) – State of the art"*, COIN Project report nº 44, SINTEF Building and Infrastructure.

Ganjian, E.; Khorami, M.; Maghsoudi, A. A. (2009), "*Scrap tyre rubber replacement for aggregate and filler in concrete*", Construction and Building Materials, V. 23, No. 5, pp. 1828-1836.

Gomes, G. J. (2013), "*Explosive Methods for Demolitions*", Centro de Investigação da Academia

Militar (CINAMIL), Academia Militar, Lisboa.

Gonçalves, M. (2015), *"Reinforcement of Reinforced Concrete with Reinforced Plaster against Explosions Actions*" (in Portuguese), Masters Dissertations in Civil Engineering, Faculty of Sciences and Technology, New University of Lisbon.

Gupta, T.; Chaudhary, S.; Sharma, R. K. (2016), "*Mechanical and durability properties of waste rubber fiber concrete with and without silica fume*", Journal of Cleaner Production, V. 112, pp. 702-711.

Kinney, G. F.; Graham, K. J. (1985), "*Explosive Shocks in Air"*, 2nd edition, Springer Berlin Heidelberg.

Lúcio, V. J. G.; Ramos, A. P. (2015), "*Notes of Concrete Structures I Subject*" (in Portuguese), Faculty of Sciences and Technology, New University of Lisbon.

Mlakar, P. F.; Barker, D. (2010), "*Handbook for Blast-Resistant Design of Buildings"*, chapter Blast Phenomena, John Wiley & Sons.

Needham, C. E. (2010), "*Blast Waves*, Shock Wave and High Pressure Phenomena", Springer Heidelberg.

Remennikov, A. (2007), "*The state of the art of explosive loads characterisation"*, Australian Earthquake Engineering Conference, pp. 1-25, University of Wollongong, Australian Earthquake Engineering Society.

UFC 3-340-02 (2014), "*Unified Facilities of Criteria: Structures to Resist The Effects of Accidental Explosions"*, Department of Defence, United States of America.

Valadares, F. and Brito, J. (2010) "Concrete with used tyre rubber aggregates: Mechanical Performance" (in Portuguese), Structural Concrete 2010, Nacional Meeting of Concrete Structures, Lisbon.